Stability of an injection-locked DFB 1.5 μm semiconductor laser

J.-Ph. Bouyer, Ch. Bréant

Classification
Physics Abstracts
42.55P — 42.60D

Stability of an injection-locked DFB 1.5 μm semiconductor laser

J.-Ph. Bouyer and Ch. Bréant

Laboratoire Lasers Ultra-Stables, E.T.C.A., 16 bis av. Prieur de la Côte d'Or, 94114 Arcueil Cedex, France

(*Received 5 December 1991, accepted 11 April 1992*)

Résumé. — La stabilité d'un laser à semiconducteur DFB à 1,5 μm verrouillé par injection est étudiée de façon systématique. Une diode laser maître à faible bruit de fréquence est utilisée pour injecter une diode laser du même type. La pureté spectrale du laser maître est intégralement transmise à la diode esclave. Une simulation numérique rend compte des résultats expérimentaux et permet d'obtenir une interprétation simple du comportement de la diode esclave. Trois régimes se manifestent à plusieurs niveaux d'injection. Le trou de relaxation apparaissant dans la plage d'accrochage, dans les cas d'injection moyenne et forte, s'interprète totalement et permet d'expliquer complètement la stabilité de la diode laser esclave. Comme conséquence, deux déterminations du facteur α de Henry [1] sont exposées, l'une d'elles avec une précision de 5 %.

Abstract. — The stability of an injection-locked DFB 1.5 μm diode laser is studied systematically. A master diode laser with high spectral purity is used to injection lock a similar diode laser. The spectral purity of the master laser is successfully transmitted to the slave diode laser. A numerical simulation fits the experimental results and gives exact simple interpretations of the behavior of the slave diode laser. Three regimes occur at different injection levels. The relaxation hole appearing on the locking range pattern, for medium and strong injection regimes, is fully explained and leads to a complete explanation of the stability of the slave diode laser. As a consequence, two possible determinations of the Henry α factor [1] are presented, with a 5 % precision for one of them.

1. Introduction.

Free-running semiconductor lasers are known to have spectral widths of the order of some tens of MHz. This corresponds to a coherence length of about 10 m, which means that they cannot be used in systems based on long distance heterodyne detection for instance. Therefore, many techniques of frequency spectrum corrections have been developed [2], such as fast electronic servo-loops [3, 4], diode lasers in extended cavities [5, 6, 7] or diode lasers coupled to high finesse external cavities [8, 9]. These techniques increase the diode laser coherence length, up to 300 km with the latter method.

Once we have obtained a master oscillator in which the frequency noise is low, it is of great

interest to transfer its spectral purity to a more powerful set of diode lasers. The aim of this paper is to investigate first optical injection methods between similar diode lasers.

This paper is divided into three parts : the complete experimental set-up is presented, with a precise description of the master diode laser with high spectral purity and of the phase measurement of the injection-locked slave diode laser. The experiments were performed with 1.5 μm DFB double channel planar buried heterostructure diode lasers, provided by Alcatel-Alsthom Recherche, France. In the second part, we consider a theoretical approach to derive a numerical simulation to fit the experimental results. The theory describes the evolutions of quantities that cannot be experimentally observed. This enables us to find out very simple laws of behavior of the injection-locked slave diode laser, as presented in the last part. The stability of the injection-locked slave diode laser is extensively studied and leads to a complete interpretation of surprising behaviors, such as the relaxation hole appearing inside the locking range.

2. Experimental.

2.1 EXPERIMENTAL ARRANGEMENT. — The experimental set-up is shown in figure 1 and is composed of three parts : a master diode laser with high spectral purity, a slave diode laser and the analysis instrumentation.

2.1.1 *The master diode laser.* — It is well known that 300 μm long diode lasers commonly have a full width at half maximum of 20-30 MHz. As explained by the Schawlow-Townes theory, this is mainly due to the short length of the cavity and a low reflection coefficient of the diode laser, which implies a photon lifetime of about 1 ps. Moreover, the frequency noise is increased by the amplitude noise through the high value of the phase-amplitude coupling factor α. As previously shown [1], this effect widens the spectral line shape of the diode laser by the factor $(1 + \alpha^2)$. Finally, the ambient acoustic noise has a dramatic effect on the linewidth and acoustic isolation of the diode lasers is necessary to obtain significant results.

The technique of optical feedback from high finesse external cavities, which we have developed [9, 10], gives a very great potential for frequency noise reduction. This method is illustrated in figure 2. A 20 cm long confocal Fabry-Perot cavity was built from Invar and employed mirrors of 99.6 % reflection coefficient and absorption plus scattering losses less than 10^{-3}. Its theoretical finesse is 390, and an experimental value of 300 was measured. The free spectral range (F.S.R.) is 375 MHz. It is used in a slightly tilted position so that the pure reflection beam can be stopped on a pin hole, to obtain a counter propagating beam with a transmission-like shape. Feedback coupling is achieved through a quarter-wave plate and a polarizer in order to adjust the amount of power sent back to the diode laser with the proper polarization. The coupling is estimated to be between − 60 dB and − 30 dB. A half-wave plate can be used to avoid polarization attenuations on the mirrors. A detector placed at the back of the confocal Fabry-Perot cavity monitors the transmission beam fringes to display the effect of the coupling as shown in figure 3. When a small modulation is applied to the current of the diode laser, a modulation of the frequency of the laser results. Without coupling (case a), the detector shows normal transmission fringes through a Fabry-Perot cavity. With coupling (case b), the peaks are dramatically widened as the frequency of the laser is held on the top of the transmission peaks. For instance, the frequency moves only about 1 MHz (the top of a transmission peak) with coupling, whereas without coupling it will shift about 1 GHz for the same modulation depth. Any static or dynamic frequency noise is therefore reduced. Hence, the full width at half maximum of the beat note between two such systems is reduced to values between 1 and 5 kHz, as shown in figure 4. This demonstrates that this technique, which we first developed at 850 nm [9] and 1 300 nm [10], is easily and fully transposable to other wavelengths such as 1 500 nm.

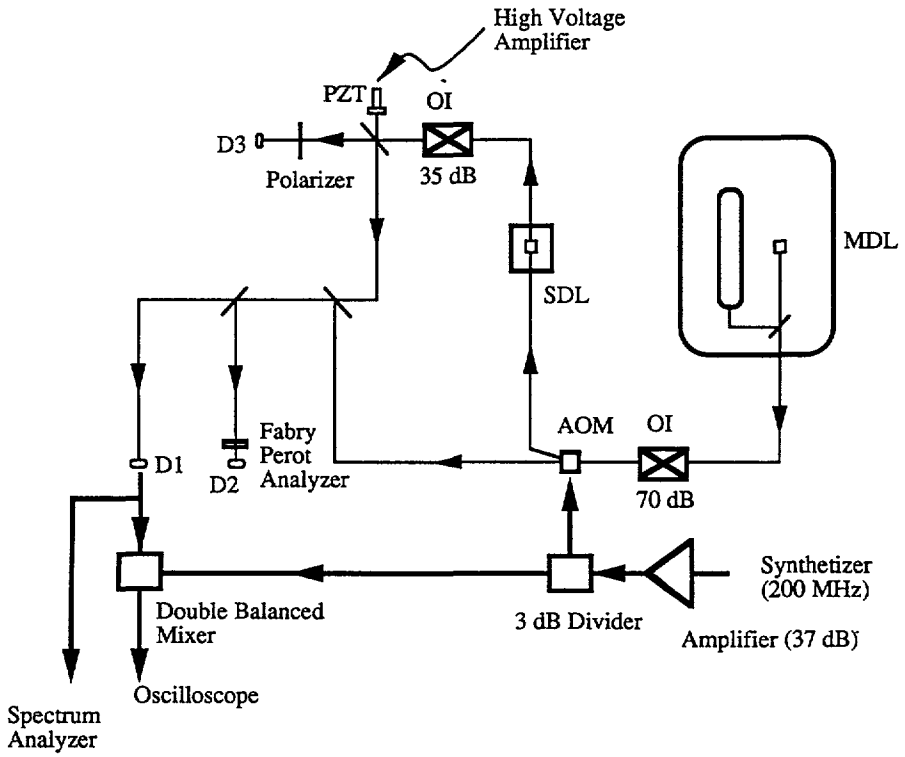

Fig. 1. — Experimental set-up. The beam from the master diode laser (MDL) is sent to the slave diode laser (SDL) *via* a 70 dB optical isolator (OI) and an acousto-optic modulator (AOM). The beat note signal between the slave diode laser and the zeroth order of the acousto optic modulator is detected on a 1 GHz bandwidth detector (D1) and is analyzed on D2 through a Fabry-Perot discriminator of finesse 380 and free spectral range 12.5 GHz. The emitted power of the injection-locked slave diode laser is measured on detector D3 through a polarizer. The 200 MHz RF power sent to the AOM comes from a frequency synthesizer and a 37 dB amplifier. A 3 dB divider is used to split the signal into one branch directed to the AOM and the other one directed to a double balanced mixer. Here, the signal is mixed with the one coming from the beat note detector and is sent to an oscilloscope. This displays the relative phase of the slave diode laser when the length of the optical path is adjusted by the mirror displacement mounted on a piezoelectric transducer (PZT) driven by a HV amplifier. The beat note signal is also sent to a high resolution spectrum analyzer.

This optical arrangement has been used to produce a laser source of high spectral quality to injection-lock a similar diode laser. The laser source of high spectral purity will now be referred to as the master diode laser.

2.1.2 *Optical injection.* — The beam from the master laser is fed through the back of a diode laser (Fig. 1). An optical isolation of more than 70 dB ensures that the master laser is not affected by any radiation from the slave laser. An acousto-optic modulator (A.O.M.) is used to monitor the injected power into the slave laser. The angular frequency ω_i of the injected beam is then the master laser angular frequency shifted by the fixed A.O.M. frequency ($\Omega/2\pi = 200$ MHz), and will be called the reference angular frequency. The detuning between the slave frequency without injection ω_0 and the reference frequency is defined by $d\omega = \omega_i - \omega_0$. It is driven by the current I_s of the slave diode laser. Focusing into the slave laser must be done with great care in order to get a sufficient number of injected photons. It is

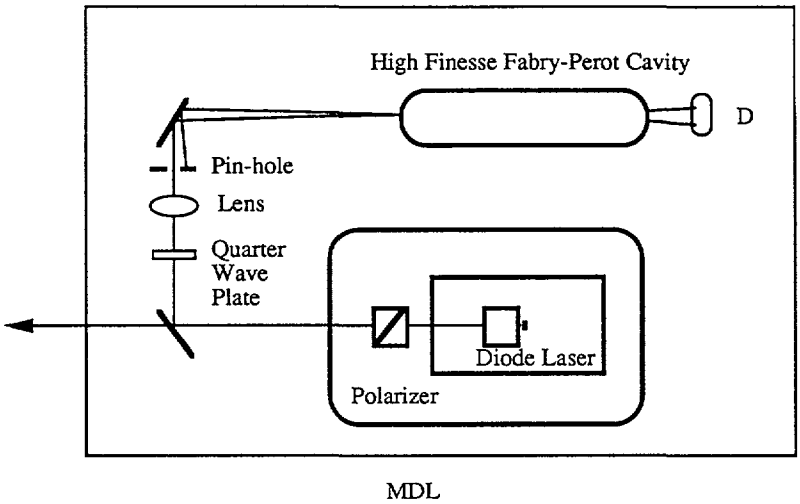

Fig. 2. — Schematic of the optical configuration employed with the master diode laser (MDL). The diode laser is optically coupled to a high-finesse cavity through a polarizer, a quarter-wave plate and a focusing lens. A detector (D) permits the transmission fringes to be monitored.

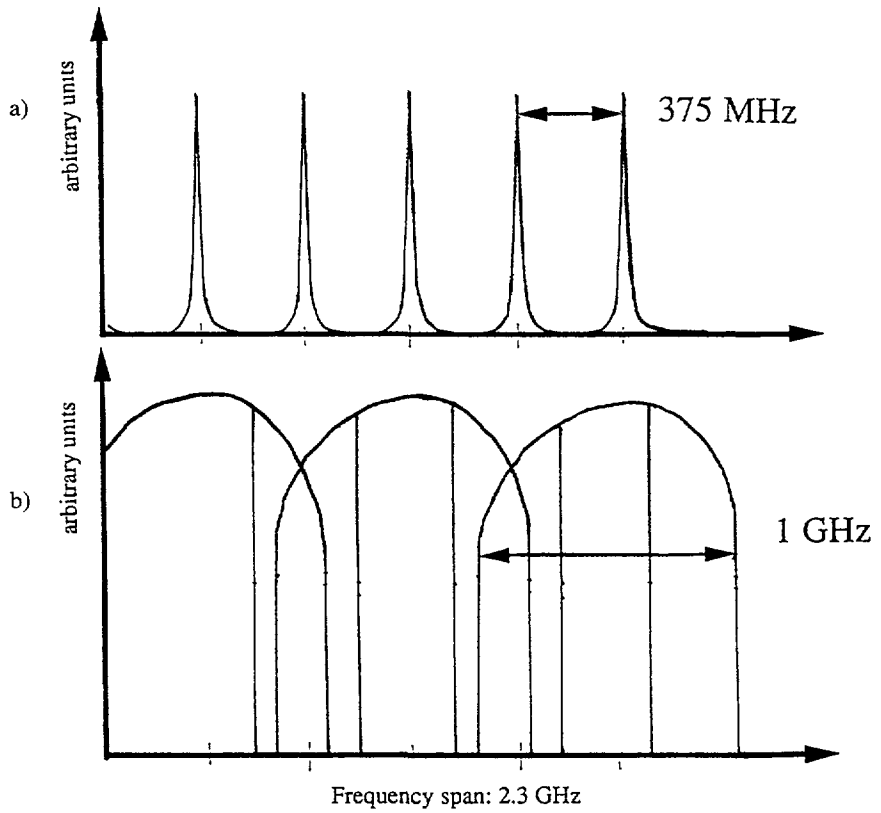

Fig. 3. — Transmission fringes of the high-finesse Fabry-Perot cavity without (a) and with (b) optical coupling. In the latter case, the diode laser remains locked on a F.P. transmission peak when a 1 GHz frequency scan is applied through a current modulation.

a)

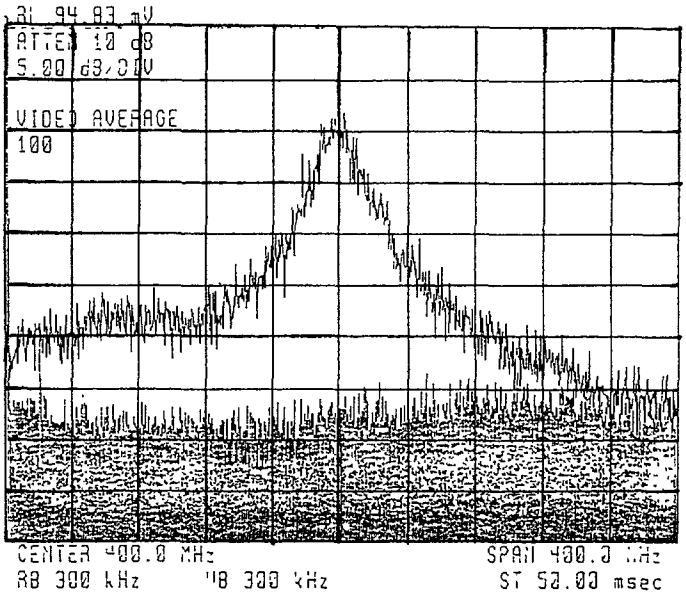

b)

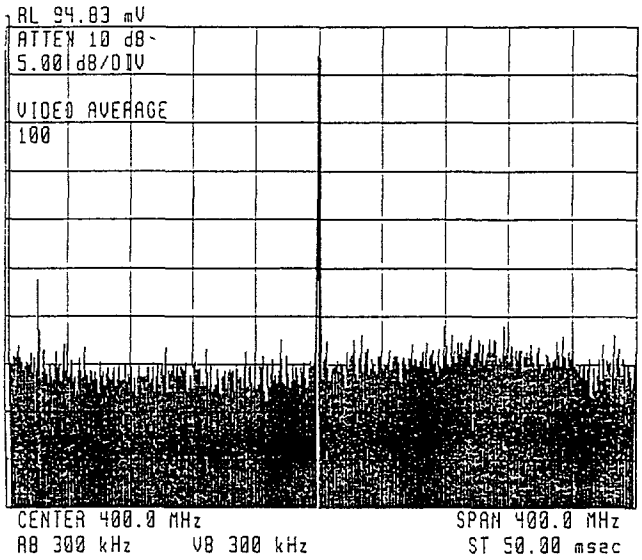

Fig. 4. — a) Frequency spectrum of a free running diode laser, the HWHM is about 20 MHz. b) Frequency spectrum of the optically coupled master diode laser, the HWHM is about 2 kHz.

necessary to get a focal point on the order of the cavity height (some tenths of a micron), with an expansion angle small enough to prevent the injected power from spreading over the other layers of the semiconductor laser. We used both a focusing lens and a gradient index rod lens to be able to reach the regimes of strong injection, as will be presented later.

2.1.3 *Analysis.* — An optical isolation of more than 35 dB ensures that no back reflections from the detectors affect the slave diode laser. The behavior of the injected slave diode laser is analyzed *via* three channels as shown in figure 1 :

— a detector (D3), behind a polarizer used as an attenuator, enables the measurement of the number of photons emitted by the slave diode laser under the various experimental conditions,

— a short Fabry-Perot cavity, of finesse 380 and F.S.R. 12.5 GHz and its detector (D2) ; this broad-band analyzer is used to identify spectral components over several GHz from the reference frequency,

— a beat note channel, to mix the beam of the injection locked slave diode laser and the zeroth order beam from the A.O.M. This channel is composed of a beam splitter and a set of lenses to match the wavefronts of both beams. The resulting beam can be sent to a broad band detector (1 GHz, D1). A spectrum analyzer (HP 70000) displays the spectrum of the beat note in the vicinity of 200 MHz, with a resolution of 30 Hz.

With these different analyses, we performed four kinds of measurements to understand the injection process :

— δP : the excess number of emitted photons due to injection. This tiny variation was deduced from the measurement of the emitted optical power with and without injection, as a function of current I_s.

— the high-resolution frequency spectrum of the beat note signal, in order to estimate the spectral purity of the injection-locked slave laser. This spectrum is centered at the A.O.M. frequency $\Omega/2\pi$.

— the amplitude of the 200 MHz frequency component of this beat note signal. This component is proportional to $\sqrt{P_{ref}} \sin(\Omega t + \theta + \psi)$, where P_{ref} is the number of photons emitted by the slave laser at the reference frequency, θ is the phase difference between the injection-locked slave diode laser and the reference beam, and ψ is an experimental phase. The amplitude measurement of this signal gives direct access to the locking range, which is the domain where the slave diode laser is frequency locked to the master oscillator.

— the phase θ was determined by mixing this beat note signal in a double balanced mixer with the 200 MHz frequency coming from the synthesizer, feeding the A.O.M. (see Fig. 1). The resulting electrical beat note is proportional to $\sqrt{P_{ref}} \sin(\theta + \psi)$. The experimental phase ψ can be varied by driving the optical path with a piezoelectric transducer (PZT). Thanks to theoretical considerations (Eq. (16)), it can be adjusted to give the phase reference for the measurements.

2.2 Experimental results.

2.2.1 *Injection locking and linewidth narrowing.* — Inside the locking range, the measurement of the width of the beat note is limited by the spectrum analyzer resolution (30 Hz), as shown in figure 5 ; the slave diode laser fully adopts the spectral purity of the coupled master laser. The reduction in frequency noise in the injection-locked slave laser can be calculated as presented in [11, 12]. Physically, this linewidth narrowing can be understood in the following way :

— a free running diode laser can be described as a spectrally white source (spontaneous emission) coupled to a spectral filter resulting from a DFB and (or) a Fabry-Perot structure. Above threshold, the spectral width of the diode laser is directly related to the width of this filter,

— the case of a diode laser injection locked by a beam of high spectral purity is entirely different : the initial photon source originates from both the broadband spontaneous emission and the spectrally sharp injected field. The latter contribution initiates the stimulated emission and depletes the gain at the reference frequency. Because of carrier scattering inside the energy band, the gain rebuilds itself at this frequency at the expense of the neighbouring frequencies. As a result, the slave laser adopts the spectral purity of the master laser.

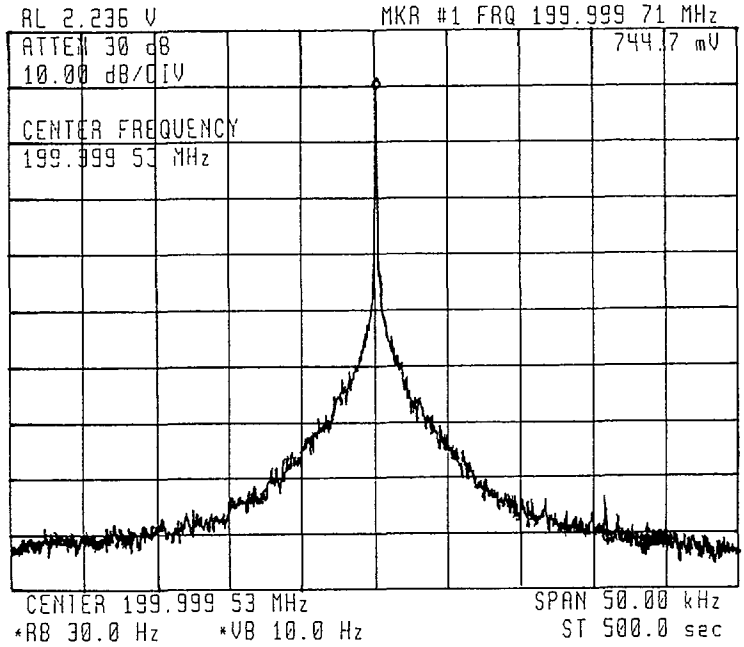

Fig. 5. — Beat note spectrum between the slave diode laser and the master diode laser. The resolution bandwidth is 30 Hz and the frequency span is 50 kHz. The vertical scale is 10 dB/Div.

The plot of the beat note amplitude *versus* detuning yields the experimental locking range, as illustrated in figure 6 for a specific injected power.

2.2.2 *Regimes of injection.* — Locking range measurements for different injection levels clearly show the existence of three regimes of injection as illustrated in figure 7 :

— a weak injection regime, where the locking range width is proportional to the square root of the injected power. The locking range width can be as high as 7 GHz for an injected power of 20 μW. In this regime, the slave laser behavior is stable ; the total optical power is

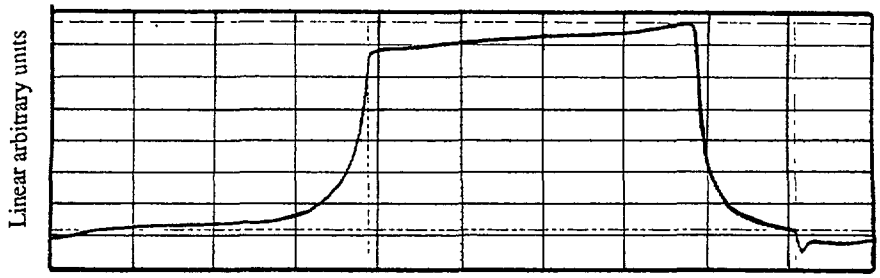

Detuning: frequency span = 10 GHz

$P_i = 5\ \mu W$

Fig. 6. — Amplitude of the beat note at 200 MHz, *versus* slave diode laser current. The curve shows the number of photons emitted at the reference frequency by the slave diode laser. Horizontal span is 10 GHz. The slightly increasing slope at the top of the pattern measures the increase of emitted photons with the diode laser current.

a)

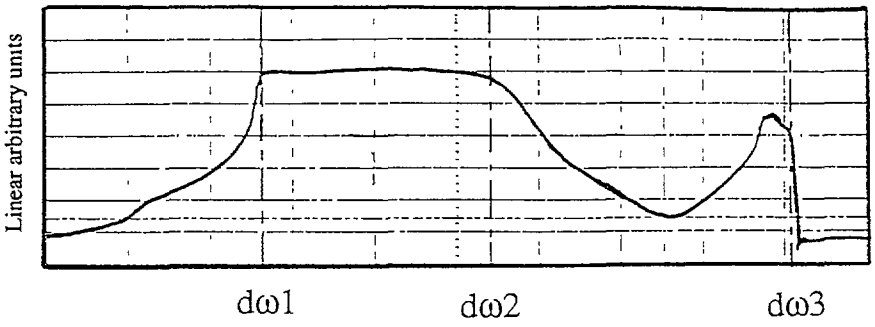

Detuning: frequency span = 14 GHz

P_i = 33 μW

b)

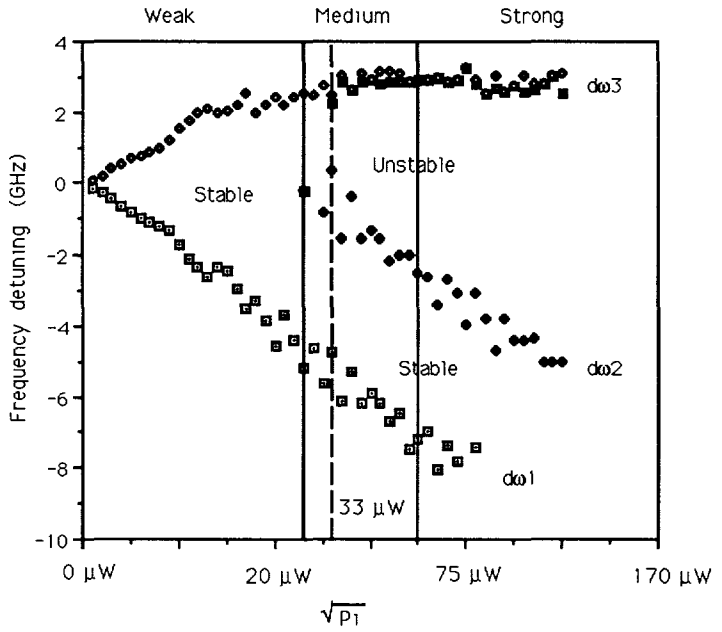

Fig. 7. — a) Experimental map of the locking range *versus* $\sqrt{P_i}$. For an injected power below 25 μW, the upper and lower dots represent the limits of the locking range. Above 25 μW, the relaxation hole appears. The vertical straight lines delimit the different injection regimes. The dotted line corresponds to figure 7b. b) Typical locking range pattern. The limits of the locking range pattern are denoted $d\omega_1$ and $d\omega_3$. The gap appearing in the right part of the locking range pattern, between $d\omega_2$ and $d\omega_3$, corresponds to instabilities in the slave diode behavior. This is the relaxation hole.

emitted at the reference frequency and the spectral purity of the master laser is perfectly transferred to the slave laser,

— a medium injection regime, where a « hole » appears inside the locking range pattern (Fig. 7). This regime is observed for injected power between 25 and 70 μW. The locking range width can become as high as 11 GHz, but only part of it (4.5 GHz) corresponds to

stable frequency locking. When the detuning is swept over the hole in the locking range pattern, sidebands are observed in the slave laser spectrum, through the multi-GHz FSR Fabry-Perot analyzer. Their position, with respect to the peak at the reference frequency, grows linearly as a function of $\sqrt{(I_s - I_{th})}$, which confirms that these instabilities are related to the presence of undamped relaxation oscillations [13] in the laser,

— a strong injection regime, where the locking range pattern is truncated because the allowed maximum oscillation amplitude is reached, as it will be demonstrated in the theoretical part.

Several experimental plots illustrating the three regimes of injection are represented in figure 8 : the locking range pattern, the evolution of sin $(\theta + \theta_0)$ and δP over the locking range. In this expression, θ_0 is defined by tan $\theta_0 = \alpha$.

It should also be pointed out that no hysteresis was observed at the border of the locking range, either by changing the detuning or the injected power.

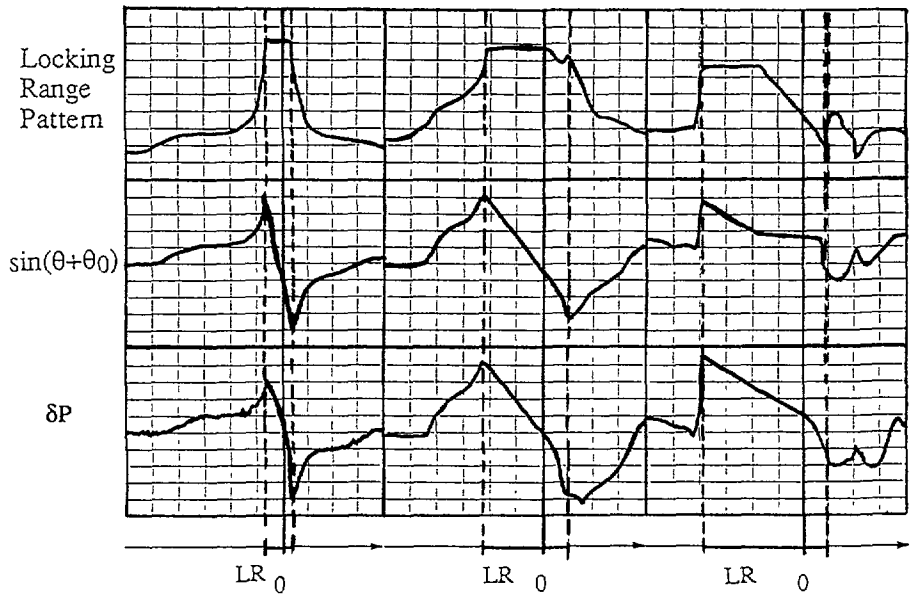

Fig. 8. — Experimental plots of the locking range pattern, sin $(\theta + \theta_0)$ and δP *versus* frequency detuning, for weak, medium and strong injection regimes. The total scan for each plot is 20 GHz. Although the units are arbitrary, the vertical scales are the same for each plot.

3. Theory.

The experimental results show that the slave laser emission is not always stationary over the whole locking range. The steady state case has been extensively studied (see for instance

Ref. [14]) and we focus our work on the unstable behavior, in order to understand the complete mechanisms of injection locking. Most of the evolution complexity is due to optical nonlinearities in the injection-locked diode laser. In order to fit the experimental results, we performed a numerical simulation of the injection-locked slave laser, based on a complete rate-equation model. Relevant hypotheses and approximations were derived from the simulation, allowing further analytical calculations and clear physical interpretations.

3.1 RATE EQUATIONS. — The temporal evolution of a diode laser can be simply described by the equation [13] :

$$\frac{\partial \mathbb{E}}{\partial t} = \mathbb{G}\mathbb{E} \tag{1}$$

where

$$\mathbb{E} = E \cdot e^{-i \cdot (\omega t + \varphi)} \tag{2}$$

$$\mathbb{G} = -i \cdot \Omega_c + \frac{1}{2} \cdot (G - \gamma) \cdot (1 - i \cdot \alpha) . \tag{3}$$

In these expressions :

E is the real amplitude of the diode laser,
ω is the angular frequency of the diode laser,
φ is the phase of the diode laser,
Ω_c is the angular frequency of the cavity resonance,
G is the diode laser gain,
γ is the diode laser loss,
α is the phase-amplitude coupling factor, $\theta_0 = \text{Arctan}\ (\alpha)$.

With optical injection, equation (1) becomes [13] :

$$\frac{\partial \mathbb{E}}{\partial t} = \mathbb{G}\mathbb{E} + K\mathbb{E}_1 \tag{4}$$

where

$$K = \frac{c}{2 \cdot \eta_g \ L_d} \cdot \frac{\sqrt{1 - R}}{R} \tag{5}$$

$$\mathbb{E}_1 = E_1 \cdot e^{-i \cdot (\omega_1 t + \varphi_1)} \tag{6}$$

In these expressions :

K is the injection strength,
E_1 is the real amplitude of the master diode laser,
ω_1 is the reference angular frequency,
φ_1 is the reference phase,
R is the intensity reflection coefficient,
η_g is the group index of the diode laser,
L_d is the length of the slave diode laser cavity.

Developing equation (4), separating real and complex parts and considering that the number of photons P inside the cavity is proportional to E^2, yields :

$$\frac{\partial P}{\partial t} = (G - \gamma) \cdot P + 2 \cdot K \cdot \sqrt{P \cdot P_1} \cdot \cos(\theta) \tag{7}$$

$$\frac{\partial \theta}{\partial t} = \Omega_c - \omega_1 + \frac{\alpha}{2} \cdot (G - \gamma) - K \cdot \sqrt{\frac{P_1}{P}} \cdot \sin(\theta) . \tag{8}$$

In these equations :

P_i is the number of injected photons stored in the cavity. In our case, $P_i = 1$ corresponds to an injected optical power of 38.4 nW,

θ is the phase difference between the injection locked slave diode laser and the reference injected beam :

$$\theta = (\omega - \omega_i) \cdot t + \varphi - \varphi_i . \tag{9}$$

The quantum treatment of the system leads to take into account in equation (7) the contribution of the spontaneous emission, in the following form :

$$R_{sp} = n_{sp} \cdot G \tag{10}$$

where n_{sp} is the number of spontaneous photons in the cavity.

The temporal evolution of the electron-hole pairs (e-h) is described by a simple rate equation :

$$\frac{\partial n}{\partial t} = \frac{I_s}{e} - \gamma_e \cdot n - G \cdot P \tag{11}$$

where

$$G = G_0 \cdot (n - n_0) . \tag{12}$$

In these expressions :

n is the number of e-h pairs inside the active layer,

n_0 is the number of e-h pairs at transparency,

G_0 is the differential gain,

γ_e is the loss of e-h pairs in the semiconductor laser.

The final system of equations is thus :

$$\frac{\partial n}{\partial t} = \frac{I_s}{e} - \gamma_e \cdot n - G \cdot P \tag{13a}$$

$$\frac{\partial P}{\partial t} = R_{sp} + (G - \gamma) \cdot P + 2 \cdot K \cdot \sqrt{P \cdot P_i} \cdot \cos(\theta) \tag{13b}$$

$$\frac{\partial \theta}{\partial t} = \Omega_c - \omega_i + \frac{\alpha}{2} \cdot (G - \gamma) - K \cdot \sqrt{\frac{P_i}{P}} \cdot \sin(\theta) . \tag{13c}$$

It is convenient to introduce

$$x = 2 \cdot K \cdot \sqrt{P_i}$$

$$P_s = \frac{\gamma_e}{G_0}, \quad \text{the saturation photon number .}$$

$$S = G_0 \cdot \left(\frac{I_s}{e} - \gamma_e \ n_0 \right), \quad \text{the source term for the gain .}$$

$d\omega_0 = \Omega_c - \omega_0$, where $\omega_0 = \Omega_c + \alpha/2(G_{wi} - \gamma) = \omega_i - d\omega$ represents the slave laser frequency without injection and G_{wi} is the gain without injection.

For typical values, $\frac{d\omega_0}{2\pi} = 1.4$ MHz.

With these notations, the rate equations become :

$$\frac{\partial G}{\partial t} = S - (P + P_s) . G_0 . G \tag{14a}$$

$$\frac{\partial P}{\partial t} = n_{sp} . G + (G - \gamma) . P + x . \sqrt{P} . \cos(\theta) \tag{14b}$$

$$\frac{\partial \theta}{\partial t} = (d\omega_0 - d\omega) + \frac{\alpha}{2} \cdot (G - \gamma) - \frac{x}{2} \cdot \frac{\sin(\theta)}{\sqrt{P}} \tag{14c}$$

3.2 NUMERICAL ALGORITHM. — The numerical resolution of the differential equation system is performed by a Runge-Kutta second-order explicit algorithm [15, 16]. The step must be chosen small compared to the period of the relaxation oscillation of the system (0.2 ns). A step which is too small however, increases calculation time and error because of the rounding errors accumulated in this case. We used a step of 1.7 ps, which is in the order of or lower than what can be found in literature [17]. The calculations in these conditions are accurate enough to perform pertinent comparisons between theory and experiment.

3.3 NUMERICAL VALUES. — First of all, we have to determine a few data corresponding to the diode lasers effectively used in the experiment :

— the laser wavelength : $\lambda = 1.52$ μm,
— the cavity length : $L_d = 300$ μm,
— the longitudinal mode spacing : $\Delta\lambda = 11.0$ Å,
— the differential power *versus* current is 0.190 W/A, yielding $dP/dI = 4.95 \times 10^6\ A^{-1}$,
— the threshold current : $I_{th} = 36.4$ mA.

Assuming an optical index $n = 3.5$, group index $\eta_g = 4$ [13] and spontaneous photon number $n_{sp} = 2$ [1], the following values are easy to derive :

— the intensity reflection coefficient : $R = 0.31$,
— the mirror loss : $a_m = 3\,919\ m^{-1}$,
— the internal loss : $a_{int} = 4\,502\ m^{-1}$,
— the total loss per second : $\gamma = 6.32 \times 10^{11}\ s^{-1}$,
— the photon lifetime : $T = 1/\gamma = 1.6$ ps,
— the number of photons stored in the cavity, without injection :

$$P_{wi} = 2.16 \times 10^5 \text{ (for an emitted power of 8.3 mW)},$$

— the corresponding steady-state gain :

$$G_{wi} = 6.32 \times 10^{11}\ s^{-1},$$

— the difference : $\gamma - G_{wi} = 5.8 \times 10^6\ s^{-1}$

The relaxation frequency was determined using the beat note with another diode laser when the slave laser is close to its threshold. Measured values clearly fit the law : $f_R = 0.75 \sqrt{I - I_{th}}$, where f_R is written in GHz and I in mA. From this measurement we derive :

— the differential gain : $G_0 = 7.1 \times 10^3\ s^{-1}$,
— the steady-state difference : $n - n_0 = 8.9 \times 10^7$,
— the e-h loss : $\gamma_e = 1.5 \times 10^9\ s^{-1}$,
— the e-h lifetime : $T_e = 0.66$ ns,
— the e-h number at transparency : $n_0 = 1.5 \times 10^8$,

— the steady-state e-h number : $n = 2.4 \times 10^8$,
— the coupling factor : $K = 3.37 \times 10^{11}\ s^{-1}$

Two important values remain to be determined, the phase-amplitude coupling factor α and the exact number of photons P_i effectively injected into the slave active layer. The numerical calculations have been performed with several values of α from 1.5 to 6 and a set of values of P_i between 0 and 6 000, which corresponds to 0-230 μW.

3.4 NUMERICAL TEMPORAL SOLUTIONS. — In figures 9 et 10 are represented the temporal evolutions of G, P and θ. Several nanoseconds are necessary for the slave diode laser to reach its steady-state regime. During this time, the energy stored in the cavity oscillates between photons and carriers at the frequency of the relaxation oscillation. In the stable part of the locking range, the phase difference between the slave and the master lasers reaches a constant steady-state value (Fig. 9a), meaning that the slave and the reference frequencies are equal. In the unstable part of the locking range, the phase after the transient regime keeps oscillating at the relaxation frequency around a constant average value (Fig. 9b). The frequency of the slave laser then equals the reference frequency, but part of the emitted power goes into relaxation oscillation sidebands. Of course, the total amplitude of phase oscillations in this case is always lower than 2 π. These calculations were used to determine the steady-state values of G, P and θ and the amplitude of their oscillations at the relaxation frequency, *versus*

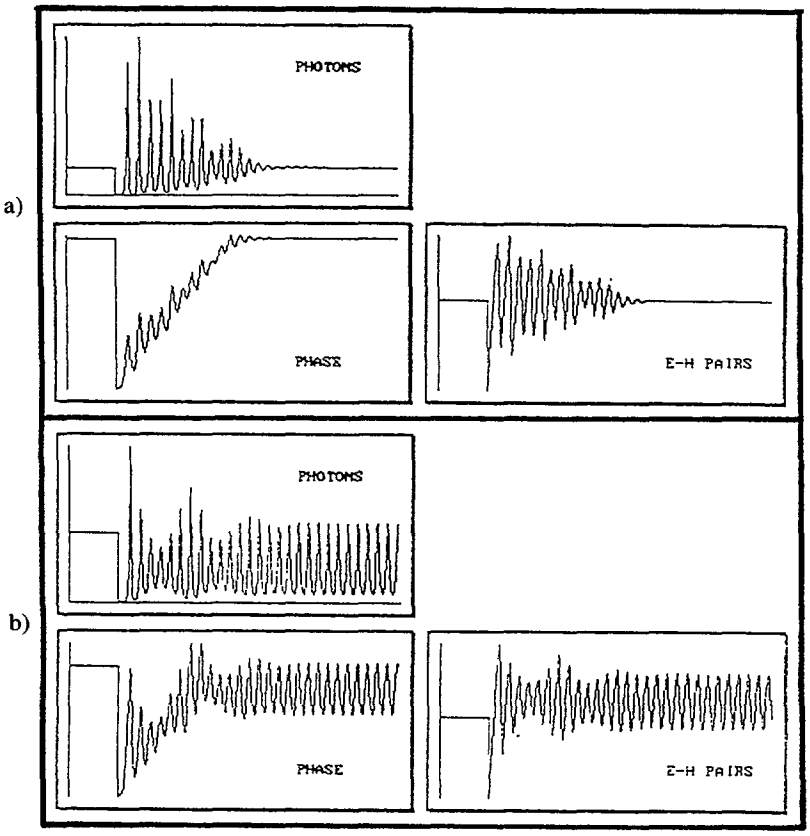

Fig. 9. — Numerical temporal solutions inside the locking range. The solutions are steady state in case a, and exhibit the relaxation oscillation at a frequency of 5 GHz in case b. The total time scale is 10 ns.

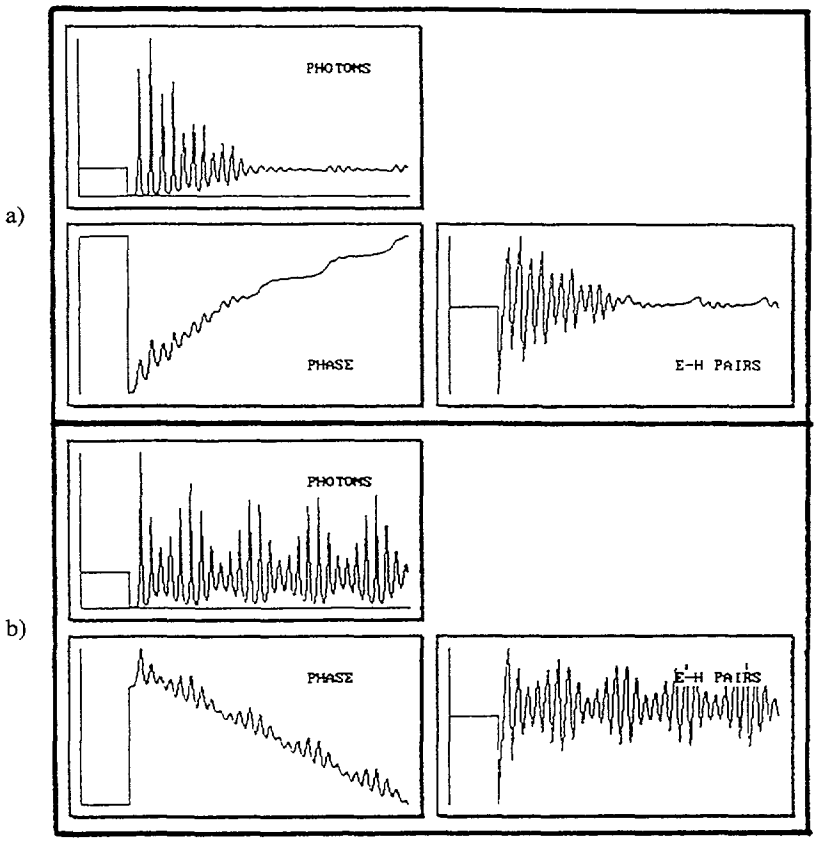

Fig. 10. — Numerical temporal solutions outside the locking range. The case a corresponds to a frequency detuning lower than $d\omega_1$ and the case b to a frequency detuning higher than $d\omega_3$. The total time scale is 10 ns.

the detuning. These simulations are in excellent agreement with the experimental results (Fig. 8). It can be noted that equation (4) is fully relevant to describe the dynamics of the injection-locked slave diode laser.

In the figures 10a and 10b, describing the situation outside the locking range, the oscillations of G, P and θ at a beat frequency close to $d\omega$ confirm the existence of population pulsations and Four-Wave-Mixing processes [18].

4. Discussion.

The experimental and numerical results highlight three injection regimes : in the weak injection regime, the solutions are stationary ; in the medium-injection regime, the locking range pattern presents a little « hole » ; in the strong injection regime, the hole grows so much that it truncates the locking range pattern.

In fact, the dynamics of the injection-locked diode laser has the following evolution, when the injection strength x varies from very low (less than $10^{11}\ s^{-1}$) to very high levels (up to $2 \times 10^{13}\ s^{-1}$) :

— For low values (on the order of $10^{11}\ s^{-1}$), the solutions are steady state. The theoretical

treatment is straightforward, but we will emphasize some points that have been misunderstood up to now.

— For medium values (on the order of $7 \times 10^{12}\ s^{-1}$), a relaxation hole appears on the right part of the locking range pattern (Fig. 7b). In this part of the locking range, the rate equation solutions oscillate at the relaxation frequency, with a maximum amplitude (in the bottom of the hole) increasing with x.

— For high values (on the order of $10^{13}\ s^{-1}$), the slave laser locking range depends critically on the phase oscillation amplitude. In fact, the injection locking range is upper-bounded by the maximum allowed value of the phase oscillation amplitude.

4.1 WEAK INJECTION REGIME. — In this section, the slave laser temporal evolution is assumed to be steady state. The behavior of the phase θ, as well as the injection-induced additional amount of gain (δG) and photons (δP), will be determined over the locking range.

4.1.1 *Behavior of the phase θ over the locking range.* — Starting from the system (14), and assuming the derivatives of G, P and θ to be zero, we obtain

$$\frac{\partial G}{\partial t} = S - (P + P_s) \cdot G_0 \cdot G \equiv 0 \tag{15a}$$

$$\frac{\partial P}{\partial t} = n_{sp} \cdot G + (G - \gamma) \cdot P + x \cdot \sqrt{P} \cdot \cos(\theta) \equiv 0 \tag{15b}$$

$$\frac{\partial \theta}{\partial t} = (d\omega_0 - d\omega) + \frac{\alpha}{2} \cdot (G - \gamma) - \frac{x}{2} \cdot \frac{\sin(\theta)}{\sqrt{P}} \equiv 0 . \tag{15c}$$

Thus :

$$\sin(\theta + \theta_0) = A - B \cdot d\omega \tag{16}$$

where

$$A = \frac{2 \cdot P \cdot d\omega_0 - \alpha \cdot n_{sp} \cdot G}{x \cdot \sqrt{P} \cdot \sqrt{1 + \alpha^2}} \tag{17}$$

$$B = \frac{2 \cdot \sqrt{P}}{x \cdot \sqrt{1 + \alpha^2}} . \tag{18}$$

In the weak injection regime, it can be checked either from the experimental plots or from the numerical simulation that $\sin(\theta + \theta_0)$ reaches the extreme values $+1$ and -1. Since $A \ll B$, the locking range appears symmetrical in this regime.

4.1.2 *Behavior of δG and δP over the locking range.* — Equation (15a) and equation (15b) lead respectively to :

$$(P_s + P) \cdot G = \text{Constant} ,$$

and

$$\frac{n_{sp} \cdot G}{\sqrt{P}} + (G - \gamma) \cdot \sqrt{P} = -x \cdot \cos(\theta) . \tag{19}$$

In particular, without injection :

$$\frac{n_{sp} \cdot G_{wi}}{\sqrt{P_{wi}}} + (G_{wi} - \gamma) \cdot \sqrt{P_{wi}} = 0 \tag{20}$$

where X_{wi} stands for « the value of X without injection ».

We define δP and δG by :

$$P = P_{wl} + \delta P \tag{22}$$

$$G = G_{wl} + \delta G . \tag{23}$$

After a first order development of equations (19) and (20), we obtain :

$$\delta G = \frac{-\sqrt{P_{wl}} . x . \cos(\theta)}{2 \cdot n_{sp} + P_{wl} + n_{sp} \frac{P_s}{P_{wi}}} \tag{24}$$

$$\delta P = \frac{\sqrt{P_{wi}} . x . \cos(\theta)}{G_{wi} \left[\frac{n_{sp}}{P_{wl}} + \frac{n_{sp} + P_{wl}}{P_{wl} + P_s} \right]} \tag{25}$$

For standard values given in 3.3, we have approximately :

$$\frac{\delta G}{G_{wi}} \approx \frac{-1}{400} \cdot \cos(\theta) \tag{26}$$

$$\frac{\delta P}{P_{wi}} \approx \frac{1}{200} \cdot \cos(\theta) . \tag{27}$$

Thus, the variation of δP or δG over the locking range in the weak injection regime leads to the determination of cos (θ). It should be noticed that δG can be positive. This result is in full agreement with our measurements, but different from what had been commonly assumed up to now.

4.2 MEDIUM INJECTION REGIME. — When the injection strength x is increased, the usual hypotheses of steady state solutions are no longer valid over the whole locking range. We will first present an explanation for the origin of the relaxation hole and then calculate the modification of the slave laser dynamics in these conditions.

4.2.1 *Origin of the relaxation hole.* — The slave laser spectrum, analyzed with a multi-GHz free spectral range Fabry-Perot, shows that, for $d\omega$ inside the relaxation hole, part of the emitted power goes into the relaxation sidebands. As previously noted, no hysteresis is found in the locking range pattern limits when $d\omega$ is swept up or down : the slave laser dynamics depends only on the static injection parameters $d\omega$ and P_i.

Let us consider the role of each term in the usual temporal system (14). When an oscillating term is present, numerical simulation shows that P and θ oscillate in phase, but in quadrature with G. This is correlated to the fact that in the equations (14b) and (14c) the predominant terms are those containing G. Thus, derivatives of P and θ are approximately proportional to G, so that θ oscillates in phase with P.

Moreover, the coefficient of sin (θ) in the last equation is in quadrature with G, which tends to slow down the resonant oscillation. Oscillations are damped as long as the sin (θ) term can compensate the G term. This is true except when $|\sin(\theta)|$ is close to 1. The case sin $(\theta) = +1$ is never reach $(\alpha \neq 0)$, therefore sin $(\theta) = -1$ corresponds to the maximum enhancement of relaxation oscillations.

4.2.2 *Dynamics of the slave diode laser in these conditions.* — In the next two parts, we shall see how the optical injection modifies the damping rate of the relaxation oscillations.

4.2.2.1 Without injection. — Let us consider equations (14) without injection :

$$\frac{\partial G}{\partial t} = S - (P + P_s)\, G_0 \,.\, G \tag{28a}$$

$$\frac{\partial P}{\partial t} = n_{sp} \,.\, G + (G - \gamma) \,.\, P \,. \tag{28b}$$

If we call δG, δP small perturbations from the steady state solutions, the following equation is readily derived :

$$\frac{\partial^2 \delta P}{\partial t^2} + 2 \cdot \Gamma \cdot \frac{\partial \delta P}{\partial t} + \Delta^2 \cdot \delta P = 0 \tag{29}$$

where :

$$\Gamma = \frac{1}{2} \cdot (\gamma - G + (P + P_s) \cdot G_0) \tag{30}$$

$$\Delta^2 = (P + P_s) \,.\, G_0 \,.\, (\gamma - G) + (n_{sp} + P) \,.\, G \,.\, G_0 \tag{31}$$

$$\Omega^2 = \Delta^2 - \Gamma^2 \tag{32}$$

Γ is the relaxation oscillation damping rate ;
Ω is the angular frequency of the relaxation oscillation.
This approach is the classical treatment for a two-body system.

4.2.2.2 With injection. — In order to determine the rate of damping of the relaxation oscillations in the medium-injection regime, we assume that the solutions of system (14) are stationary, and consider small variations around these solutions ; the rate equations (14) can be linearized :

$$\frac{\partial \delta G}{\partial t} = -(P + P_s) \,.\, G_0 \,.\, \delta G - G_0 \,.\, G \,.\, \delta P \tag{34a}$$

$$\frac{\partial \delta P}{\partial t} = (n_{sp} + P) \,.\, \delta G - (\gamma - G) \,.\, \delta P - x \,.\, \sqrt{P} \,.\, \sin(\theta) \,.\, \delta\theta \tag{34b}$$

$$\frac{\partial \delta \theta}{\partial t} = \frac{\alpha}{2} \cdot \delta G + \frac{x \,.\, \sin(\theta)}{4 \,.\, P^{3/2}} \cdot \delta P - \frac{x \,.\, \cos(\theta)}{2 \,.\, \sqrt{P}} \cdot \delta\theta \,. \tag{34c}$$

The numerical simulation shows that no modification of the damping rate Γ occurs when α is set to 0 in system (14). It indicates that the term $\frac{\alpha}{2} \cdot (G - \gamma)$ in the phase equation (14c) is responsible for the injection-induced modification of Γ. Besides, in the small oscillation case, a first order development in x for the evolution of δP is justified, and leads to the equation :

$$\frac{\partial^2 \delta P}{\partial t^2} + 2 \cdot \Gamma' \frac{\partial \delta P}{\partial t} + \Delta'^2 \, \delta P = 0 \tag{35}$$

where

$$\Delta'^2 = \Delta^2 + \frac{x \,.\, \Gamma \,.\, \alpha \,.\, G_0 \,.\, G \,.\, \sqrt{P} \,.\, \sin(\theta)}{\Delta^2} \tag{36}$$

$$\Gamma' = \Gamma + \frac{1}{4} \cdot \frac{\alpha \,.\, x \,.\, \sqrt{P} \,.\, G_0 \,.\, G}{\Delta^2} \cdot \sin(\theta) \tag{37}$$

are calculated from the diagonalization of system (34).

Since $\Delta^2 \approx PGG_0$, we have approximately :

$$\Gamma' \approx \Gamma + \frac{1}{2} \cdot \frac{\alpha \,.\, K \,.\, \sqrt{P_1}}{\sqrt{P}} \cdot \sin(\theta) \tag{38}$$

$$\Omega' \approx \Omega + \frac{\alpha \,.\, K \,.\, \Gamma}{2 \,.\, \Omega} \cdot \sqrt{\frac{P_1}{P}} \cdot \sin(\theta) \,. \tag{39}$$

Equation (38) shows that the damping rate is minimum for $\theta = -\pi/2$. Considering the solutions of $\Gamma' = 0$, with relation (16), gives the frequency boundaries of the relaxation hole.

The case where $\Gamma' < 0$ must be understood as a regime where oscillations are sustained and do not diverge exponentially. The reason comes from the nonlinear terms preventing the growth of the oscillations that are not taken into account in the simple linear model developed here.

4.3 STRONG-INJECTION REGIME. — In this case, the locking range splits into two parts : the left part, in which the solutions remain steady state and the right part, in which they exhibit an important relaxation oscillation component.

It appears from the numerical simulation that the evolution of G, E and θ in the strong injection regime can be approximately described by the functions :

$$G = G_1 + G_2 \,.\, \cos(\Omega \,.\, t) \tag{40a}$$

$$E = E_1 + E_2 \,.\, \sin(\Omega \,.\, t) \tag{40b}$$

$$\theta = \theta_1 + \theta_2 \,.\, \sin(\Omega \,.\, t) \tag{40c}$$

where G_i, E_i, θ_i are constant.

Considering only the oscillations at Ω, we derive

$$P = E^2 = \left(E_1^2 + \frac{E_2^2}{2}\right) + 2 \,.\, E_1 \,.\, E_2 \,.\, \sin(\Omega t) \,. \tag{41}$$

The temporal system (14) is equivalent to :

$$\frac{\partial G}{\partial t} = S - (P + P_s) \,.\, G_0 \,.\, G \tag{42a}$$

$$\frac{\partial P}{\partial t} = n_{sp} \; G + (G - \gamma) \cdot P + \frac{x}{2} \cdot E \cdot \cos(\theta) \tag{42b}$$

$$\frac{\partial \theta}{\partial t} = (\mathrm{d}\omega_0 - \mathrm{d}\omega) + \frac{\alpha}{2} \cdot (G - \gamma) - \frac{x}{2 \,.\, E} \cdot \sin(\theta) \,. \tag{42c}$$

For small values of θ_2, these equations can be developed using Bessel functions of the first kind :

$$\cos(\theta_2 \,.\, \sin(\Omega \,.\, t)) \approx J_0(\theta_2)$$

$$\sin(\theta_2 \,.\, \sin(\Omega \,.\, t)) \approx 2 \,.\, J_1(\theta_2) \,.\, \sin(\Omega \,.\, t) \,.$$

Collecting the terms proportionnal to $\cos(\Omega t)$ in the last two equations, we obtain :

$$\Omega^2 = G_0 \,.\, G_1 \,.\, \left(n_{sp} + E_1^2 + \frac{E_2^2}{2}\right) \tag{43}$$

$$\theta_2 \,.\, \left(n_{sp} + E_1^2 + \frac{E_2^2}{2}\right) = \alpha \,.\, E_1 \,.\, E_2 \,. \tag{44}$$

In the case of small oscillations ($E_2 \approx 0$), Ω represents the usual relaxation oscillation. Expression (44) yields

$$E_2 = \frac{\alpha - \sqrt{\alpha^2 - 2 \cdot \theta_2^2}}{\theta_2} \cdot E_1 \tag{45}$$

which gives the limit of the allowed amplitude of the phase oscillation θ_2 as :

$$\theta_{2\,\max} = \frac{\alpha}{\sqrt{2}} .$$

The limit calculated by the numerical simulation (with $\alpha = 3$) is 2.12.

The limiting value $\theta_{2\,\max}$ is never reached in the medium injection regime. At the transition between the medium and strong injection regimes, the amplitude of the phase oscillation at the bottom of the relaxation hole does reach the value $\theta_{2\,\max}$. In the strong injection regime, the locking range has an upper limit determined by the frequency detuning for which θ_2 reaches $\theta_{2\,\max}$.

4.4 SUMMARY OF THE DIFFERENT CASES. — Let us sum up, in figure 11, the three cases found in theoretical calculation : the weak, the medium and the strong injection regimes. These theoretical plots were only calculated inside the locking range and should thus be compared with the measurements performed over the same range (Fig. 8).

4.5 APPLICATION TO THE DETERMINATION OF THE HENRY α FACTOR. — The Henry α factor of a free-running diode laser cannot be determined, because the working point (G, P) of the laser is independent of θ. This is entirely different in the presence of external coupling. For instance, the influence of α can be observed under frequency modulation [19], with feedback from an external cavity [20], or with an injection locking technique [21].

The above developments provide two different methods to determine α : the former from static solutions of the injection locked slave diode laser and the latter from its dynamic behavior.

A complete study of these two methods has been realized and will be described in a next paper [22]. Here we give a quick overview of the principles.

a) *α from static solutions of the injection locked slave diode laser :* This method is similar to the one presented in [21]. Previously, in the weak injection regime, we saw that inside the locking range, δP is proportional to $\cos(\theta)$ as a function of $d\omega$ (Eq. (25)), whereas $\sin(\theta + \theta_0)$ varies as $-d\omega$ (Eq. 16)). Comparison of the two curves leads to the values of θ_0, and $\alpha = \tan(\theta_0)$. The main difficulty comes from the small value of δP compared to P which implies that great care must be exercised in the signal-to-noise ratio analysis.

With this method, we have measured $\alpha = 2.5(+/-0.1)$ for an injection current of $I_s = 100$ mA ($I_{th} = 35$ mA).

b) *α from dynamic behavior of the injection locked slave diode laser :* This method of determination is based on the variations of both the left boundary of the locking range and the bottom of the relaxation hole with $\sqrt{P_i}$, in the medium-injection regime. Under specific experimental conditions, the ratio of the slopes of plots *versus* $\sqrt{P_i}$ yields $\sqrt{1 + \alpha^2}$. This determination leads to $\alpha = 2.8(+/-0.5)$ for $I_s = 100$ mA ($I_{th} = 35$ mA).

It might be noted that this second method of determination does not have such a good precision but is in the order of those commonly found in publications [19-21].

	INJECTION REGIMES		
	Weak	Medium	Strong
Comments	- Symmetrical locking range.	- Non symmetrical locking range. - Little relaxation hole	- The locking range is truncated, because the maximum allowed oscillation is reached.
Locking range (arbitrary units) versus detuning	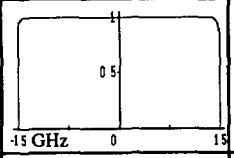	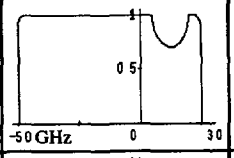	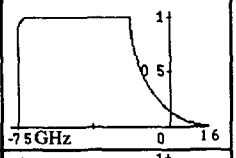
sin(θ+θo)	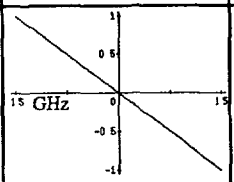	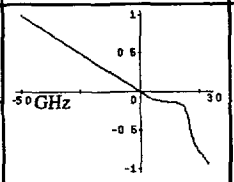	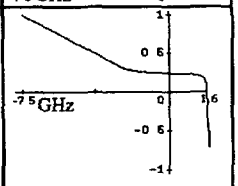
sin(θ)	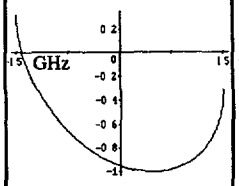	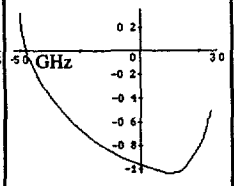	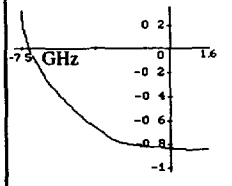
cos(θ)	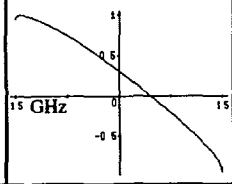	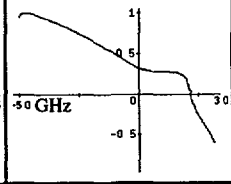	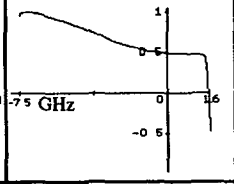
Dynamics	Everything is steady state	- The relaxation hole is a perturbation - In the hole, oscillations are not damped.	On part of the locking range, solutions are steady state; on the other part, they oscillate at the relaxation frequency.

Fig. 11. — Summary of the characteristic parameters calculated over the locking range in the three injection regimes. The frequency spans are given in GHz on the horizontal axes. Vertical scales are linear and in arbitrary units.

5. Conclusion.

In this paper, we have presented both an experimental and a theoretical analysis of the stability of injection locked DFB 1.5 μm semiconductor lasers.

We found that, inside the locking range, the slave diode laser adopts the frequency and the spectral purity of the master laser. We established that three regimes of injection have to be considered :

— a weak injection regime, where the locking range width is proportional to the square root of the injected power. The locking range can be as high as 7 GHz for an injected power of 20 μW ;

— a medium injection regime, where a hole is appearing inside the locking range pattern. In our case, this occurs for injected power between 25 and 70 μW. The locking range width may be as high as 11 GHz, but only part of it (4.5 GHz) corresponds to stable frequency locking, with the total power emitted at the reference frequency ;

— a strong injection regime, where the locking range pattern is truncated because the maximum allowed oscillation amplitude is reached.

Numerical simulations based on the rate equations of the injected slave laser were performed and successfully compared to the experimental records. A few data that are impossible to get from the experiment, such as temporal evolutions of the gain, of the number of emitted photons and of the relative phase of the injection locked slave diode laser, were easy to plot from the simulation. In addition, it enabled us to find out assumptions which allowed us to achieve simple analytical calculations.

The main conclusions of this systematic study are :

— in the weak injection regime, the locking range pattern is quasi symmetrical ;

— in the medium injection regime, a relaxation hole appears in the locking range pattern. The limits of this hole can be deduced from calculation of the damping rate of the relaxation oscillations. The bottom of the relaxation hole corresponds to $\theta = -\pi/2$;

— in the strong injection regime, the undamped relaxation oscillations truncate the locking range pattern, when the amplitude of the phase oscillation reaches the maximum allowed value $\theta_{2\,\max} = \dfrac{\alpha}{\sqrt{2}}$.

Finally, we mentioned two methods to determine the Henry α factor for an injection-locked laser.

Work on multimode systems and high power diode laser arrays are now in progress.

6. Post-deadline note.

Recent investigations show that the two methods presented for the determination of α are not fully relevant. Another method based on the measurement of gain variation due to injection locking is in good agreement with a measurement based on modulation technique [23]. All details and explanations can be found in [22, 24, 25].

Acknowledgement.

The authors are grateful to A. Clairon (Laboratoire Primaire du Temps et des Fréquences, Paris), J. Hare (Ecole Normale Supérieure, Paris) and A. Aspect (Institut d'Optique Théorique et Appliquée, Orsay) for stimulating discussions. They specially thank P. Schanne and J.-P. Foing (Laboratoire Lasers Ultra-Stables) for judicious corrections to this article. They also thank M. Dudas and M. Matabon (Alcatel-Alsthom Recherche), for providing the diode lasers. This work was supported by the Direction des Recherches, Etudes et Techniques.

References

[1] HENRY C. H., *IEEE J. Quantum Electron.* **QE-18** (1982) No. 2, February.

[2] WIEMAN C. E. and HOLLBERG L., « Using diode lasers for atomic physics », *Rev. Sci. Instrum.* **62** (1991) No. 1, January.

[3] OHTSU M. and KOTOJIMA S., *IEEE J. Quantum Electron.* **QE-21** (1985) 1905.

[4] SAITO S., NILSSON O. and YAMAMOTO Y., *Appl. Phys. Lett.* **46** (1985) 3.

[5] FLEMING M. W. and MOORADIAN A., *IEEE J. Quantum Electron.* **QE-17** (1981) 44.

[6] DE LABACHELERIE M., « Principales Caractéristiques des Lasers à Semiconducteurs à Cavité étendue », Doctoral Thesis, Orsay, France, February (1988).

[7] DE LABACHELERIE M. and CEREZ P., « An 850 nm Semiconductor Laser Tunable over a 300 A Range », *Opt. Commun.* **55** (1985) 174-178.

[8] DAHMANI B., HOLLBERG L. and DRULLINGER R., *Opt. Lett.* **12** (1987) 876-878.

[9] LAURENT P., CLAIRON A. and BRÉANT C., *IEEE J. Quantum Electron.* **QE-2** (1989) No. 6, June.

[10] BOUYER J. P., BRÉANT C., LAURENT P. and CLAIRON A., « Injection Locking of 1.26 μm Multimode Semiconductor Lasers », to be published in TENICOLS'91 proceedings, Font-Romeu, June (1991).

[11] SAITO S. and MOGENSEN F., « Effective Bandwidth for FM Noise Suppression in an Injection-Locked Semiconductor Laser », *Electron. Lett.* **21** (1985) No. 24, November.

[12] SPANO P., PIAZZOLLA S. and TAMBURRINI M., « Frequency and Intensity Noise Injection-Locked Semiconductor Lasers : Theory and Experiments », *IEEE J. Quantum Electron.* **QE-22** (1986) No. 3, March.

[13] AGRAWAL G. P. and DUTTA N. K., « Long-Wavelength Semiconductor Lasers » (Van Nostrand Reinhold) Chapter 6.

[14] PETITBON I., GALLION P., DEBARGE G. and CHABRAN C., *IEEE J. Quantum Electron.* **QE-24** (1988) No. 2, February.

[15] FORSYTHE G. E., MALCOLMAND M. A. and MOLER C. B., « Computer Methods for Mathematical Computations », Prentice-Hall (1977).

[16] DAHLQUIST G. and BJORCK A., « Numerical Methods », Prentice-Hall (1974).

[17] SCHUNK N. and PETERMANN K., *IEEE J. Quantum Electron.* **QE-22** (1986) No. 5, May.

[18] AGRAWAL G. P., « Population Pulsations and Nondegenerate Four-Wave Mixing in Semiconductor Lasers and Amplifiers », *J. Opt. Soc. Am. B* **5** (1988) No. 1, January.

[19] HARDER C., VAHALA K. and YARIV A., « Measurement of the Linewidth Enhancement Factor α of Semiconductor Lasers », *Appl. Phys. Lett.* **42** (1983) No. 4, February.

[20] ACKET G. A., LENSTRA D., DEN BOEF A. J. and VERBEEK B. H., « The Influence of Feedback Intensity on longitudinal Mode Properties and optical Noise in Index-guided Semiconductor Lasers », *IEEE J. Quantum Electron.* **QE-20** (1984) pp. 1163-1169, October.

[21] HUI R., D'OTTAVI A., MECOZZI A. and SPANO P., *IEEE J. Quantum Electron.* **QE-27** (1991) No. 6, June.

[22] BOUYER J. P., SCHANNE P. and BRÉANT C., « Determination of the Henry α factor in 1.5 μm diode laser through injection locking techniques », to be published.

[23] DUDA and GABRIAGUES, Alcatel-Alsthom Recherche, private communication, June 1992.

[24] BOUYER J.-P. and BRÉANT C., « Relaxation oscillation analysis of an injection-locked diode laser », PTh081 in the proceedings of the IQEC'92 (Vienna, June 14-19, 1992).

[25] BOUYER J.-P., « Stabilisation par injection d'un laser à semi-conducteur », Doctoral Thesis, Orsay, France, June 1992.